Progress Towards the Miniaturization of an Ultrasonic Scalpel for Robotic Endoscopic Surgery Using Mn:PIN-PMN-PT High Performance Piezocrystals

Nicola Giuseppe Fenu*, Nathan Giles-Donovan*, Xuan Li*, Zhu Liang†, Abdul Hadi Chibli*, Haosu Luo†
Chris Stock‡, Shujun Zhang§, Margaret Lucas* and Sandy Cochran*
*Centre for Medical and Industrial Ultrasonics, James Watt School of Engineering, University of Glasgow, G12 8QQ, UK
Email: nicola.fenu@glasgow.ac.uk
†Shanghai Institute of Ceramics, Chinese Academy of Sciences, Shanghai, China
‡School of Physics and Astronomy, University of Edinburgh, EH9 3JZ, UK
§ISEM, Australian Institute for Innovative Materials, University of Wollongong, NSW 2500, Australia

***Abstract*—Mn:PIN-PMN-PT piezocrystals are under consideration for potential use in miniaturised ultrasonic scalpels for robotic minimally-invasive surgery where small size and light weight may be advantageous. Electromechanical coupling coefficient $k > 0.9$ was calculated for both for both [001] and [011] poled Mn:PIN-PMN-PT was calculated, confirming the well-recognized higher efficiency of this material when compared to standard piezoceramics. Novel transducer design strategies have been explored, and outcomes are discussed. The introduction of components with additional compliance in a standard $\mathbf{d}_{31}$ mode transducer has been shown to drop the resonant frequency of the first longitudinal mode by more than 17%, with more than 75% improvement in tip/blade displacement. Results suggest that the combination of high performance piezocrystals with highly compliant components may be a useful route to follow to achieve our miniaturisation target.**

I. Introduction

Robotic endoscopic surgery (RES) is increasingly used in minimally invasive procedures, where smaller surgical tools are necessary to access laparoscopic ports 5 or 10 mm in diameter. The Da Vinci® system (Intuitive Surgical Inc., Sunnyvale, CA, USA) is a popular RES platform, with three arms dedicated to functional instruments and tissue manipulation, and one arm carrying a 3D endoscope. One of the most recent innovations in the Da Vinci® system is the EndoWrist® , which enables 7 degrees of freedom (DOF) at the end-effector, replicating the process of open-surgery.

Several electrosurgical energy instruments, both monopolar and bipolar, are available with EndoWrist® joints. However, ultrasonic scalpels that are EndoWrist® -compatible do not exist, limiting the application of such tools in several medical procedures.

This work was supported by *Ultrasurge, Surgery Enabled by Ultrasonics*, funded by the Engineering and Physical Sciences Research Council (EPSRC), EP/R045291/1. Nathan Giles-Donovan is sponsored by EPSRC/Thales UK iCASE Award No. EP/P510506.

Several electrosurgical energy instruments, both monopolar and bipolar, are available with EndoWrist® joints. However, ultrasonic scalpels that are EndoWrist®-compatible do not exist, limiting the application of such tools in several medical procedures. Conventionally, soft-tissue ultrasonic scalpels operate at 55 kHz, where the large vibration of the blade induces cutting and coagulation due to frictional heating of the tissue against another non-vibrating, grasping jaw. To date, the Harmonic ACE® (Ethicon Endosurgery, Somerville, NJ, USA) is the only ultrasonic device compatible with the Da Vinci® system. Specifically, to accommodate its dimensions, the ultrasonic actuator is placed outside the human body, and a long wave-guide drives the vibration towards the end-effector. The device is axially constrained with the robotic arm, allowing only rotation and longitudinal movements. Moreover, the wave-guide (shaft) undergoes high vibrational stresses, which can result in excess heating (>200 °C), thus requiring more precautions in manoeuvering to prevent undesired injuries.

Several advantages have been reported in ultrasonic cutting/cauterisation when compared with conventional electrosurgical devices. These include: more precise dissection margins, reduced thermal damage spread, and faster tissue and vessel coagulation. These advantages often contribute to reducing the overall procedure time and faster patient recovery through reductions in intra- and post-operative complications. Hence, it is attractive to consider how to increase the use of ultrasonic energy devices in RES [1]-[5].

One way to achieve this goal is through the development of a wrist-like ultrasonic scalpel. This requires reduction in the transducer diameter and length. Conventionally, ultrasonic scalpels, adopt the Langevin design first introduced in the early years of the 20^{th} century. In this design, a back mass and a front mass sandwich a stack of piezoelectric rings constrained by a pre-stressing bolt. The axial dimensions determine the resonant frequency of the longitudinal mode of the device [6].

TABLE I
PIEZOELECTRIC MATERIALS FOR HIGH POWER APPLICATIONS

Material	Symmetry	Mode (i,j)	d_{ij} (pC/N)	k_{ij}	Q_{ij}	$k_{ij}^2 Q_{ij}$
PZT4	6mm	3,3	300	0.7	500	245
PZT8	6mm	3,3	230	0.64	1000	410
Mn:PIN-PMN-PT	mm2	3,3	1053	0.9	1000	900
	4mm	3,3	1200	0.9	800	648

Several strategies are under investigation to reduce transducer dimensions. These include the use of Generation III piezocrystals (Mn:PIN-PMN-PT), combined with the exploration of different vibrational modes (d_{33}, d_{31}, d_{32}), and novel concepts embedding folded and high-compliance components. Mn:PIN-PMN-PT relaxor-PT piezocrystals also offer a way forward as their higher efficiency and energy density may reduce the volume and weight of the drive components in smaller tools.

In this paper we report a study of energy conversion at microscopic and macroscopic scales using finite element analysis – FEA – (OnScale, Glasgow, UK) to model the length-thickness-extensional (LTE) modes of Mn:PIN-PMN-PT. Preliminary results in transducer miniaturisation are also reported, with both FEA and early physical prototype designs.

II. HIGH PERFORMANCE PIEZOCRYSTALS

Table I reports material properties [7]-[9] and compares conventional hard, high-drive PZT-4 and PZT-8 piezoceramics with Mn:PIN-PMN-PT piezocrystals in the mm2 and 4mm symmetries. The figure of merit high power applications, represented by $k^2 Q_{ij}$ originates from Stansfield [10]. Based on this, Mn:PIN-PMN-PMT in the length-extensional (so-called 33) mode has a figure of merit considerably higher than that of PZT. However, because of limited availability, there is still a paucity of use in practical applications.

A. Higher Energy Density

In high power applications, high energy density is very valuable. This can be interpreted in practical terms by energy conversion, which is quantified by the electromechanical coupling coefficient, k. However, k is usually linked with resonant vibrational mode geometries which obscure the inherent response of the material. In order to decouple the material's piezoelectric response from resonance phenomena, we can consider a generalized k, defined at zero frequency. The electromechanical coupling factor is defined as

$$k^2 = \frac{\text{Converted energy}}{\text{Input energy}}. \quad (1)$$

In the absence of stress ($\nabla \cdot T = 0$ under static excitation) and under an electric field applied in the 3 direction, this can be rewritten as

$$k^2 = \frac{d_{i3} c_{ij}^E d_{j3}}{\epsilon_{33}^T}, \quad (2)$$

where d_{i3} is the piezoelectric charge coefficient, c^E is the stiffness, ϵ^T is the dielectric permitivitty at constant strain and summation convention is assumed (i, j run $1-6$). The inclusion of the summations fully incorporates the material anisotropy and quantifies all conversion mechanisms allowed by symmetry.

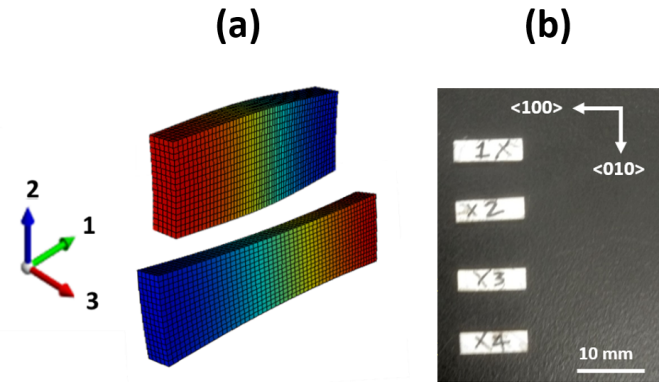

Fig. 1. **(a)**: Example of Length-Thickness-Extensional mode in FEA, and **(b)**: LTE d_{31} mode plates.

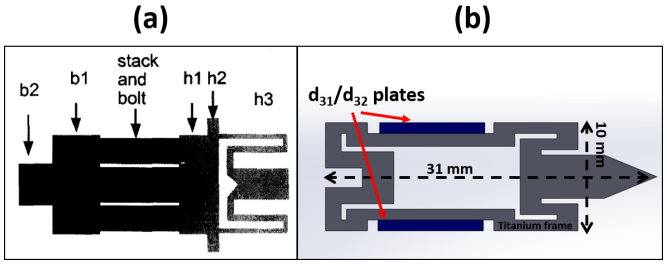

Fig. 2. **(a)**: double folded horn design [2], and **(b)**: folded d_{31} planar transducer.

B. Mn:PIN-PMN-PT

LTE plates, with dimensions of $l = 10t$, and $w = 3t$, where l is the length, t is the thickness, and w is the width, have a fundamental vibrational mode when poled along the thickness which makes them expand and contract lengthwise, as shown in Fig. 1(a). When Mn:PIN-PMN-PT piezocrystals are poled along [001], macrosymmetry 4mm, the LTE mode is commonly referred to as the d_{31}-mode and is identical with the d_{32}-mode, with Fig. 1(b) showing d_{31}-mode plates considered in this work. However, when Mn:PIN-PMN-PT plates are poled along [011], macrosymmetry mm2, the d_{31} and d_{32} coefficients are different, with the latter being higher. The LTE plate geometry thus offers more versatility in terms of design possibilities than conventional rings employed in bolted Langevin-style transducers (BLTs). For this reason it is useful to assess its suitability for power ultrasonics applications.

III. MINIATURISATION STRATEGIES

Along with the choice of Mn:PIN-PMN-PT piezocrystals, with very high material performance, modifications of conventional transducer designs are needed.

A. Folding

Folded structures, as shown in Fig. 2(a), were introduced by Sherrit for aerospace applications. This particular patented

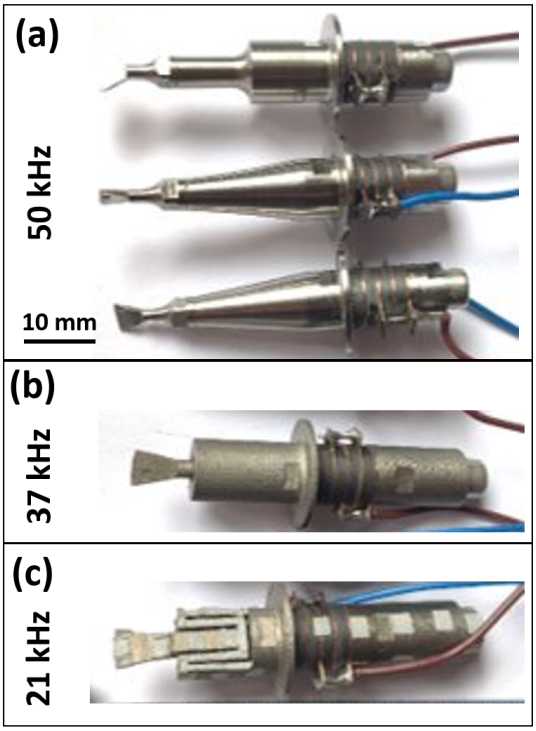

Fig. 3. **(a)**: 50 kHz transducers with different horn geometries, **(b)**: 37 kHz folded d_{33} transducer, and **(c)**: 21 kHz folded d_{33} planar transducer.

TABLE II
COMPARISON OF ENERGY DENSITY QUANTIFIED BY THE GENERALIZED k^2 IN PIEZOMATERIALS

Material	Symmetry	Geometry	Generalized k	
			Calculated	FEA
PZT4	6mm	3,1	0.6806	0.6805
Mn:PIN-PMN-PT A	4mm	3,1	0.9154	0.9154
Mn:PIN-PMN-PT B	mm2	3,1	0.9223	0.9223
		3,2	0.9223	0.9223

design, has the capability of lowering the resonant frequency of the longitudinal mode of a transducer of a given length [11], [12]. The effect of different horns on 50 kHz BLTs has been explored, as shown in Fig. 3(a). Complete, Fig. 3(b), and planar, Fig. 3(c), folded horn structures have been studied, showing, respectively, 13 kHz and 29 kHz reductions in the frequencies of the first longitudinal mode. Fig. 2(b) shows a potential configuration of the folded structure in a planar d_{31} device with FEA demonstrating the first longitudinal mode located at approximately 20 kHz. However, high values of electrical impedance at resonance, of the order of several $k\Omega$, were also present.

B. d_{31} and d_{32} components

From (3), where l is the length, E is the Young's modulus, and ρ is the material's density, it is possible to obtain the frequency of the first longitudinal vibational mode ($f_{n=1}$) of a thin rod. From (3) it is also clear that longer the rod, the lower $f_{n=1}$.

$$f_{n=1} = \frac{1}{2l}\sqrt{\frac{E}{\rho}} \tag{3}$$

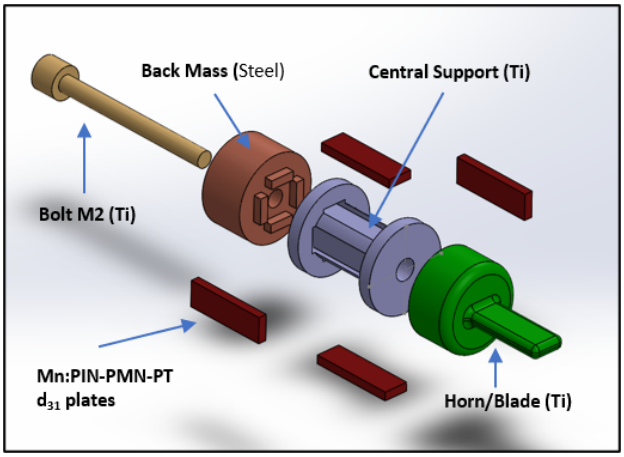

Fig. 4. Exploded view of *'Solid-Solid'* d_{31} mode transducer in standard configuration with four LTE plates.

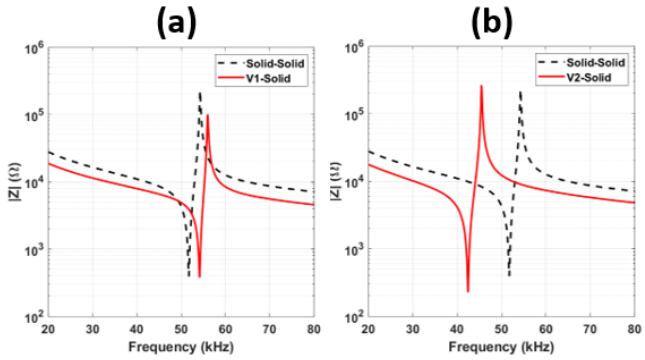

Fig. 5. Simulated electrical impedance change for different d_{31} mode transducers compared to Solid-Solid, as **(a)**: Solid-Solid vs V1-Solid, **(b)**: Solid-Solid vs V2-Solid.

Fig. 4 presents a conceptual design ("Solid-Solid"), embedding four LTE Mn:PIN-PMN-PT d_{31} mode plates, where dimensions have been tuned accordingly for the first longitudinal mode to be at approximately 50 kHz with a length less than in a conventional device.

IV. RESULTS

Table II compares the generalized k for two compositions of Mn:PIN-PMN-PT against PZT-4. It shows the calculated value from (2) validated against FEA (OnScale) for a 1 mm $\times$ 3 mm $\times$ 10 mm d_{31} or d_{32} plate. Excellent agreement was found and this result has been found, independent of geometry.

Table III presents measured material properties from d31 mode plates from the Shanghai Institute of Ceramics, Chinese Accademy of Science (SICCAS, Shanghai, China).

In addition measured properties are reported for d_{32} mode plates of two types, from TRS Technologies ("Type 1", TRSX4B-HQ, TRS Technolgies, PA, USA) and from SICCAS

TABLE III
MEASURED PROPERTIES OF d_{31} AND d_{32} PLATES OF MN:PIN-PMN-PT

Symmetry	**Type**	**Mode** (i,j)	$\mathbf{d}_{33}$ (pC/N)	$\mathbf{k}_{ij}$	$\mathbf{Q}_{ij}$
4mm	/	3,1	-700	0.4	500
mm2	1	3,2	-800	0.81	1000
mm2	2	3,2	-2100	0.92	350

TABLE IV
SIMULATED DEVICES PERFORMANCE

Model	$\mathbf{f}_r$ (kHz)	$\mathbf{Z}_{min}$ Ω	$\mathbf{k}_{eff}$ /	$\mathbf{Q}_{eff}$ /	**dsp @50** $\mathbf{V}_{PP}$ μm
Solid-Solid	51.7	395.1	0.31	260	6.9
V1-Solid	54.1	386.3	0.26	250	5.8
V2-Solid	42.4	232.1	0.38	240	12.3

("Type 2"). Type 2 d_{32}-mode plates have shown extremely high k and high d coefficients whereas Type 1 shows very high Q_m, with reasonably high k. In all cases, the d_{32} mode has shown great potential over the d_{31} mode. Simulated electrical impedance of d_{31}-mode transducers are presented in Fig. 5. These are from concept devices, Fig. 5, with parts modified, Fig. 5(a) and substituted, Fig. 5(b). The overall length of these devices has not been changed but the resonant frequency is reduced. Table IV shows simulated device properties and maximum tip/blade displacement extracted in steady-state conditions. No large changes were found in the electrical impedance values at resonance and both k_{eff} and Q_{eff} were similarly stable.

V. CONCLUSIONS AND FUTURE WORK

Mn:PIN-PMN-PT piezocrystal has been shown to be a potential candidate to design power ultrasonics transducers. The generalized electromechanical quality factor presented in Section II B, demonstrates its higher energy density compared to conventional ultrasound materials, such as PZT-4. This also supports the possibility to have a smaller device, where the same performance may be achieved with a lower volume of material, especially when combined with the d_{31} and d_{32} modes. Future work will involve the fabrication of different prototypes combining d_{31}- and d_{32}-mode Mn:PIN-PMN-PT piezocrystals with other components in order to investigate the effects of resonant frequency on blade/tip displacement and soft-tissue cutting performance.

REFERENCES

[1] M. Kroh, *"Essentials of Robotic Surgery"*, M.Kroh S. Chalikonda Ed. Springer, Switzerland, 2015. DOI: https://doi.org/10.1007/978-3-319-09564-6.

[2] G. Spinoglio, *"Robotic Surgery Current Applications and New Trends.*, G.Spinoglio Ed. Springer-Verlag, Switzerland, 2015. DOI: https://doi.org/10.1007/978-88-470-5714-2.

[3] Velotti, N., Manigrasso, M., Lauro, K. Di, Vitiello, A., Berardi, G., Manzolillo, D., Anoldo, P., Bocchetti, A., Milone, F., Milone, M., Palma, G. D. De, Musella, M., "Comparison between LigaSure and Harmonic in Laparoscopic Sleeve Gastrectomy : A Single-Center Experience on 422 Patients", *Hindawi, Journal of Obesity*, Article ID 3402137, pp. 1-5, 2019. DOI: https://doi.org/10.1155/2019/3402137.

[4] Devassy, R., Krentel, H., Verhoeven, H. C., Torres-de, L. A., De Wilde R. L., "Laparoscopic ultrasonic dissectors : technology update by a review of literature.", *Dovepress, Medical Devices: Evidence and research*, 2019.

[5] Yang, S. C., Ahn, J., Kim, J. H., Yi, J. W., Hur, M. H., Lee, K., "Comparison of the vessel sealer Extend with harmonic ACE in robotic bilateral axillary-breast approach thyroid surgery", *Gland Surgery*, vol. 9, no. 2, pp. 164-171, 2020. DOI: https://doi.org/10.21037/gs.2020.01.18.

[6] Lucas, M., Mathieson, A., *"Ultrasonic cutting for surgical applications"*, in Power Ultrasonics: Applications of High-Intensity Ultrasound, Elsevier Ltd. https://doi.org/10.1016/B978-1-78242-028-6.00023-5

[7] Zhang, S., Li, F., Jiang, X., Kim, J., Luo, J., Geng, X., "Advantages and challenges of relaxor-PbTiO3 ferroelectric crystals for electroacoustic transducers. A review", *Progress in Materials Science*, no. 68, pp. 1–66, 2015. DOI: https://doi.org/10.1016/j.pmatsci.2014.10.002.

[8] Zhang, S., Shrout, T. R., "Relaxor-PT single crystals: Observations and developments", *IEEE T-UFFC*, vol. 57, no. 10, pp. 2138–2146, 2010. DOI: https://doi.org/10.1109/TUFFC.2010.1670.

[9] Sahul, R., "Effect of Manganese Doping on PIN-PMN-PT crystals for High Power Applications", *PhD Thesis*, The Pennsylvania State University, 2014.

[10] Stansfield, D., Elliott, A., *"Underwater Electroacoustic Transducers: Second Edition"*. Peninsula Publishing, 2017.

[11] Sherrit S., Badescu M., Bao X., Bar-Cohen Y., Chang Z., *Novel horn designs for power ultrasonics*, IEEE Ultrasonics Symposium, 10.1109/ultsym.2004.1418291, 2004.

[12] Sherrit S., Askins S. A., Gradziol M., Dolgin B. P., Bao X., Chang Z., Bar-Cohen Y., "Novel horn designs for ultrasonic/sonic cleaning, welding, soldering, cutting, and drilling", *Proceedings of SPIE - The International Society for Optical Engineering*, 10.1117/12.474671, 2002.